



Evaluation of Different Water Indices for Extraction Surface Water of AL-Hawizeh Marsh from Landsat 8 Imagery

Zahraa Abd Ali*

Department of Civil Engineering, College of Engineering, University of Basrah, Basrah, Iraq
[*Corresponding author]

Wisam A. Alawadi

Department of Civil Engineering, College of Engineering, University of Basrah, Basrah, Iraq

Wisam S. Al-Rekabi

Department of Civil Engineering, College of Engineering, University of Basrah, Basrah, Iraq

Abstract

The Al-Hawizeh marsh, situated in southern Iraq, and it is one of the largest wetlands in the region. This study aims to identify the best method for obtaining the water surface area of Al-Hawizeh marsh using Landsat 8-OLI imagery. Five techniques are tested and evaluated based on their performance in extracting water surface area: normalized different water index (NDWI), modified normalized different water index (MNDWI), normalized different vegetation index (NDVI), normalized different moisture index (NDMI), and water index refers to short wave infra-red (RSWIR). The results demonstrate the superiority of the MNDWI technique, which achieves an overall accuracy of approximately 87.04% and a kappa coefficient of 0.792. It is recommended that this technique be applied in areas with similar conditions to efficiently extract surface water area from Landsat 8 OLI data.

Keywords

Al-Hawizeh marsh, Landsat 8, Extraction of water surface, Water indices

INTRODUCTION

Non-coastal, above-ground, open fresh or brackish waterbodies, such as rivers, reservoirs, lakes, and wetlands, play a crucial role in the fluctuations global carbon cycles, consequently the climate, and they give an essential asset to all living organisms on the planet [1]. Changes in water bodies affects other natural resources, ultimately influencing the ecological community.

The field measurement of wetlands flows in its natural location is a main method for Observation and studying wetland. These measurements enable a comprehensive view of surface water accessibility, but they require a large quantity of labor and financial resources. Consequently, it is necessary to explore alternative methods for monitoring surface water.

Remote sensing has emerged as a vital source of data for analyzing changes in various earth resources, with a particular emphasis on surface water [2]. Remote sensing serves as a fundamental approach to obtaining spatial data. It involves the assessment of electromagnetic radiation interactions with both the atmosphere and various objects [3].

Multiband methods generate from remote sensing, also known as water-index methods, have demonstrated significant potential in various studies. Their effectiveness in detecting water, their cost-effectiveness, and their user-friendly nature contribute to their appeal.

One of the most significant challenges that the marshes of Iraq are currently facing is the combination of Water shortage, drought, and the lack of water-sharing agreements with neighboring countries pose significant challenges. Furthermore, the water quality in the rivers of Tigris and Euphrates is deteriorating due to the presence of sewage and industrial pollutants, as well as saltwater intrusion from the Arabian Gulf [4].

A series of spectral indices are developed for observing and supervising dynamic changes in large surface water bodies, including wetlands.

The indices include the NDVI (normalize different vegetation index)[5]. NDWI (normalize different water index)[6]. To mitigate the noise from urban areas, a modified water index called MNDWI was introduced by substituting the NIR band with the shortwave-IR (SWIR) band, building upon the foundation of NDWI. [7]. NDMI (normalize different moisture index) [8]. Water Index (WI), referred to as RSWIR. This index is particularly useful for detecting water bodies and changes in water levels, as well as for monitoring vegetation health and crop stress [9].

A recent study by Yousif and Al-Saedi study the alterations in Al-Hammar and Central marshes were investigated in this study. The dataset obtain from Google Earth data-engine was utilized, which offers the most comprehensive and specific information regarding marshes mapping through the implementation of the average spatial resolution of a satellite images, like Landsat and Sentinel. The analysis involved the use of sensors Landsat 5, 7, and 8, and a total of 10802 scenes were examined and filtered. The objective was to obtain the normalized difference water index MNDWI through a specialized code within the GEE environment [10].

A study by AHMED, Bushra A., and Tabarak S The water level in the southern marshlands was estimated following the flood waves by using satellite image classification.

This work aims to compare the land use in Al-Hawizah marshes before and after the flood season. Furthermore, it seeks to determine the water reflectivity values for the years 2018 and 2019. The calculation of water reflectivity values was based on Landsat-8 images taken between March 4, 2018 and March 7, 2019, both before and after the floods that impacted the southern marshlands.. The results indicate that remote sensing is capable of identifying water and determining its size and boundaries [11].

The purpose of current work was to investigate the accuracy of remote sensing methods frequently used for mapping and extracting water bodies, specifically focusing on the Al-Hawizeh wetland which had experienced multiple droughts. This comparative research will analyze the optimal effective index for mapping Al-Hawizeh marsh and its findings can be extrapolated to similar regions and Determine which water extraction index are best.

STUDY AREA

Al-Hawizeh marsh is a significant marsh in the southern region of Iraq. It serves as a habitat for birds and fish, making it a crucial source for fishing and agricultural activities situated between longitudes 47°21'30.1"E – 47°52'34"E and latitudes 31°17'12.8"N – 31°47'31.8"N, to the east of the Tigris River [13], covering an approximate area of 2400Km² - 3000Km² with water levels ranging from 1.5 to 5 meters (Fig. 1). The climate is mild, with an average yearly temperature of 37.7° Celsius, an annual rainfall of 400-1000 millimeters, and a mean relative humidity of 49 percent. By 2003, this area had shrunk to less than 7% of its 1973 size, which was 8,926 Km² within Iraq [12].

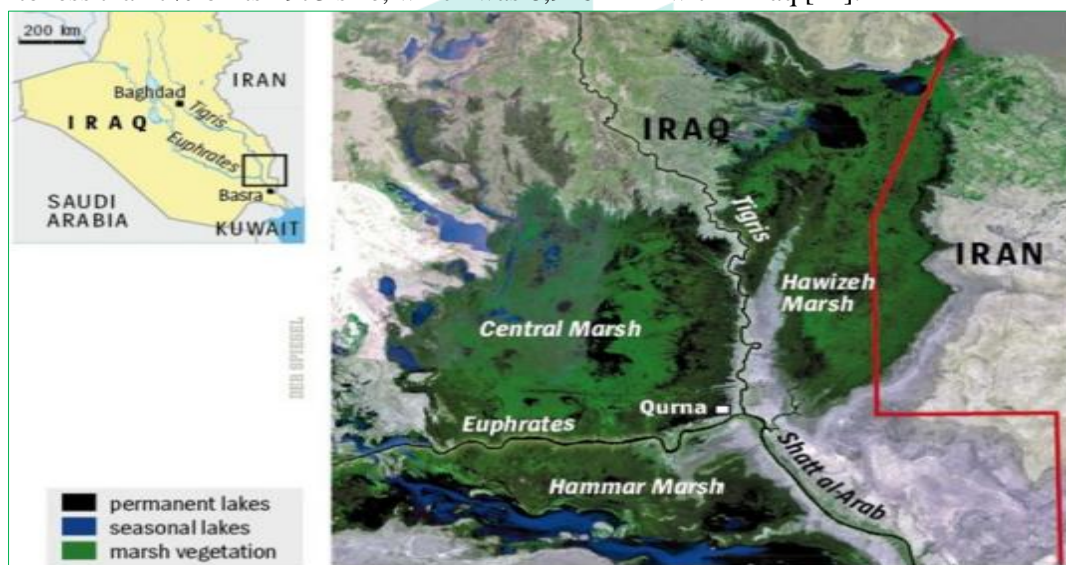


Fig. 1 Marsh lands of Iraq [12]

During the hot summer season, temperatures tend to rise significantly, leading to low rates of rainfall. As a result, many marshes in Iraq including AL-Hawizeh marsh end up either partially or completely dried, ultimately leading to a decrease in the total flooded marsh areas. Temperature rainfall fluctuations play a crucial role in altering the environment of the AL-Hawizeh marsh [13].

IMAGE DATA

Landsat 8-OLI is the source of remote sensing data that was used. The Landsat 8-OLI is a versatile, high-fidelity imaging system capable of capturing detailed, multi-spectral data across a broad swath of 190 kilometers. This advanced satellite was deployed in February 2013, marking a significant milestone in Earth observation technology, it captures global imagery over eleven spectral bands. The satellite offers a panchromatic band at 15 m spatial resolution, eight bands at 30 m, and two bands at 100 m as shown in (Table 1). The data was obtained from the website (<http://earthexplorer.usgs.gov>). Details are reported in reference [14].

Table 1 Characteristics of Landsat 8-OLI Satellite Bands: Centre Wavelengths and Spatial Resolutions [14]

Landsat 8-OLI			
Spectral band	Band name	Wavelength (µm)	Resolution (m)
B1	Coastal Aerosol	0.443	30
B2	Blue	0.482	30
B3	Green	0.561	30
B4	Red	0.655	30
B5	NIR	0.865	30
B6	SWIR-1	1.609	30
B7	SWIR-2	2.201	30
B8	Panchromatic	0.590	30
B9	Cirrus	1.373	15
B10	TIR-1	10.895	30
B11	TIR-2	12.005	100

For this research, we utilize the Level-2 product "Surface Reflectance" from the Landsat satellites between 2016 and 2023, ensuring that atmospheric corrections have been applied.

The bands that used in this research were (B3, B4, B5, B6) which means (green, red, near infra-red, short wave infrared) because these bands are required to calculate the water indices which were utilized in our study. To avoid the presence of clouds, we deliberately did not upload the image in the winter and the table shows the (Table 2.) shows the dates for uploading the image.

Table 2 Dates of available Landsat 8 satellite images for the Hawizhe marsh between 2013 and 2023

Landsat 8-OLI	
The year	Month and day
2016	2 June
2017	11 October
2018	26 July
2019	29 July
2020	16 August
2021	31 May
2022	6 August
2023	30 June

METHODOLOGY

Method Outline and Image Pre-Processing

To accomplish the objectives of this study, the following steps were undertaken: The boundaries of the area of interest were clearly defined, relevant data was gathered from various sources, the images were processed to enhance their quality, the area of water surface was obtained from each image using a water index. To extract the water surface area in each image when applying a water index for water extraction, the water threshold was manually selected to ensure accurate results. Fig. 2 illustrates the overall methodology employed in this study to detect changes in water surface area.

A series of pre-processing steps were executed in order to make the input satellite images ready:

The atmospheric correction together with radiometric calibration procedures were performed in accordance with the methods described in [15]. All data which were utilized in this study were made from level 2 so that we didn't make this correction and this had no impact on the results.

Description of Water Extraction Techniques

Normalized Difference Vegetation Index (NDVI)

The NDVI is commonly utilized as an index for monitoring vegetation, encompassing all green vegetation. It is derived from an amalgamation of red and NIR bands and can be calculated using the familiar equation (Eq. 1) by Rouse et al. (1974).

$$NDVI = \frac{(NIR - RED)}{(NIR + RED)} \quad (1)$$

Normal vegetation displays diminished reflectivity in the visible portion of the electromagnetic spectrum, as it absorbs pigments such as chlorophyll. Conversely, it exhibits enhanced reflectivity in the NIR region. The numerical values of this parameter span a scale from -1 to 1. Values between -1 and 0 indicate positive elements like barren land, urban areas, and water bodies, whereas values from 0 to 1 signify vegetative cover characteristics [16].

Normalized Difference Water Index (NDWI)

The NDWI is a metric employed to track alterations in water bodies by leveraging the spectral signatures of the green and near-infrared (NIR) bands. This index can be calculated using the formula developed by McFeeters in 1996 (Eq. 2) [16].

$$NDWI = \frac{(GREEN - NIR)}{(GREEN + NIR)} \quad (2)$$

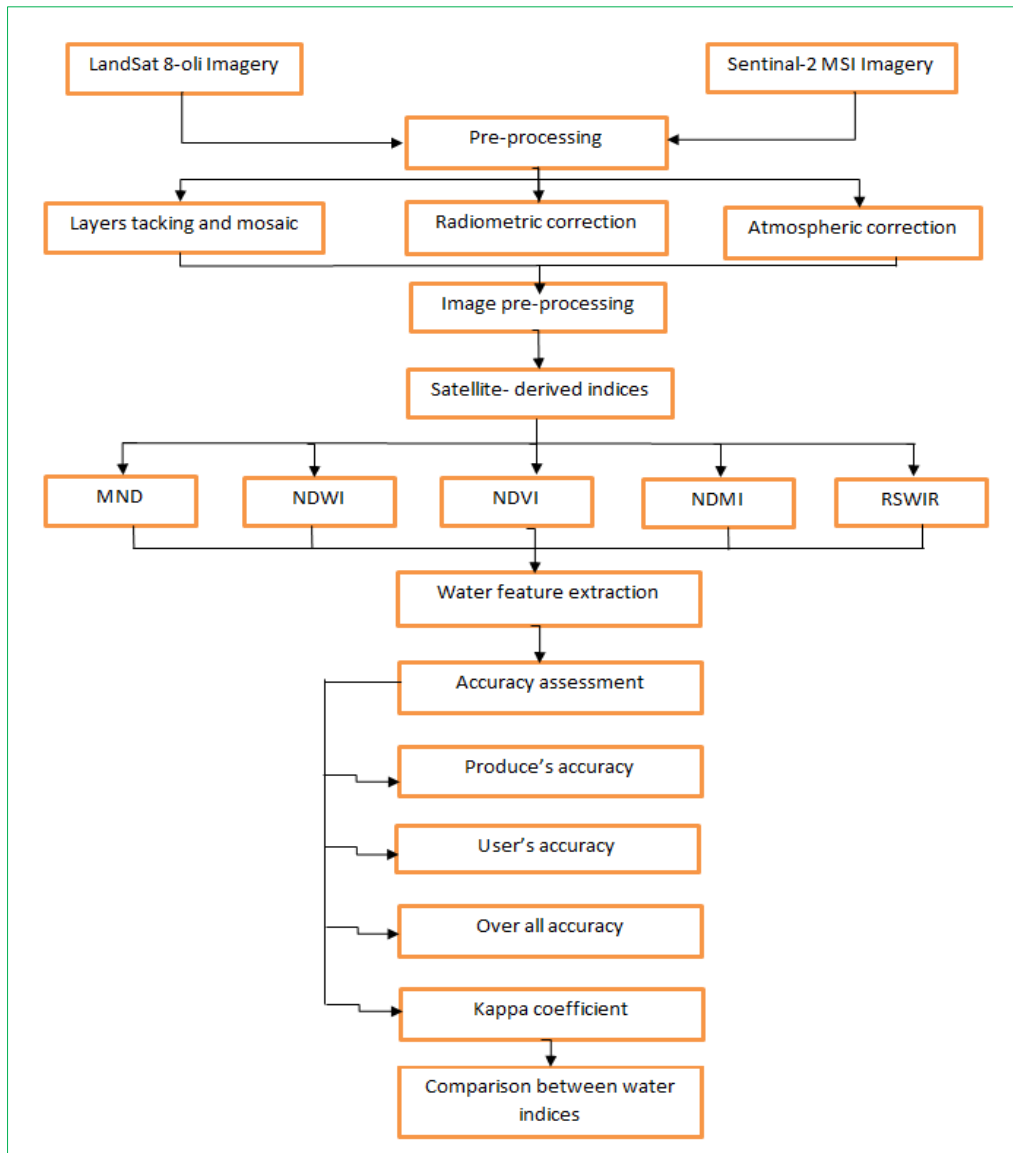


Fig. 2 Process for Extracting Water Bodies and Mapping Land Cover

Modified Difference Water Index (MNDWI)

The MNDWI approach proposed by [17], it has been widely adopted and is an effective index for extracting water bodies. It is represented by Eq (3).

$$\text{MNDWI} = \frac{(\text{GREEN} - \text{SWIR})}{(\text{GREEN} + \text{SWIR})} \quad (3)$$

The water bodies exhibit elevated values due to their enhanced reflectivity in the green spectral range compared to the red spectral range, whereas non-water features display diminished NDWI values. By establishing a specific cutoff point for the MNDWI, such as a straightforward value of zero, it is possible to categorize the MNDWI results into two distinct groups: water and non-water features.

Normalized Difference Moisture Index (NDMI)

NDMI is calculated by Eq. (4) where the NIR is Landsat -8 Band 5 and the mid-infrared (MIR) or (SWIR) is Landsat-8 Band 6.

$$\text{NDMI} = \frac{(\text{NIR} - \text{SWIR})}{(\text{NIR} + \text{SWIR})} \quad (4)$$

This index is commonly referred to as the NDMI, although the term "moisture" is more conventional and retained for lack of a more precise term. One reason a universally accepted term is lacking is that the biophysical interpretation of indices that incorporate MIR bands is more challenging than those that only utilize red and NIR bands. The value of this index ranging between -1 to 1, where water body has positive value [8].

Water Index (RSWIR)

This Index defined by (Rogers and Kearney (2004)), referred to as Red and Short Wave Infra-Red (RSWIR) and can be calculated by Eq.(5)[9].

$$\text{RSWIR} = \frac{(\text{RED} - \text{SWIR})}{(\text{RED} + \text{SWIR})} \quad (5)$$

Its numerical value ranging between -1 to 1, where water body have positive value.

We used B3, B4, B5, B6 because we need it in calculating the indices for the Image from Landsat.

In this context, the NDWI, NDMI, MNDWI, RSWIR, and NDVI indexes were computed from Landsat 8 images to assess their efficacy for extracting surface water. A land-water threshold was manually applied to categorize the images into two classes, land and water. Optimal land-water thresholds for each index were identified through trial and error and comparison to reference maps generated through visual interpretation [18].

Water Threshold Selection

When employing a spectral water index to delineate water features from surrounding land areas in remote sensing imagery, it is crucial to judiciously select an optimal threshold value that best separates water from non-water pixels. Analysis of the unique spectral signature of water reveals that it exhibits very low reflectance in the infrared portion of the electromagnetic spectrum, while displaying relatively higher reflectance in the visible wavelengths. By leveraging this distinct spectral characteristic of water, we can compute a water index that accentuates water details and suppresses land features in the remote sensing image. The ideal scenario is to set the water index threshold at 0, where all positive values are classified as water and negative values are considered as land [19].

To distinguish between arid land and vegetation, we use a trial and error method to choose the appropriate threshold. The threshold value chosen in image classification must give a classification that is close to reference map. Comparison is made between the image after classification and the reference map through the Google Earth Pro or composite image. If there is a large difference, we try to change the threshold value so that the Image is closer to reality. Therefore, in some indices, we did not use the value 0, as we used (0.03, 0.08, 0.09) as shown in the (Table 3) but the most commonly used value is 0.

Table 3 The threshold that used for the indices

Landsat-8		
Index	Date of Image	Threshold
NDWI	2/6/2016	0
MNDWI	2/6/2016	0
NDMI	2/6/2016	0.09
NDVI	2/6/2016	0
RSWIR	2/6/2016	0
NDWI	11/10/2017	0
MNDWI	11/10/2017	0
NDMI	11/10/2017	0.08
NDVI	11/10/2017	0
RSWIR	11/10/2017	0
NDWI	26/7/2018	0
MNDWI	26/7/2018	0
NDMI	26/7/2018	0.08
NDVI	26/7/2018	0
RSWIR	26/7/2018	0
NDWI	29/7/2019	0
MNDWI	29/7/2019	0
NDMI	29/7/2019	0.03
NDVI	29/7/2019	0
RSWIR	29/7/2019	0
NDWI	16/8/2020	0
MNDWI	16/8/2020	0
NDMI	16/8/2020	0.03
NDVI	16/8/2020	0
RSWIR	16/8/2020	0
NDWI	31/5/2021	0
MNDWI	31/5/2021	0
NDMI	31/5/2021	0
NDVI	31/5/2021	0
RSWIR	31/5/2021	0
NDWI	6/8/2022	0
MNDWI	6/8/2022	0
NDMI	6/8/2022	0.09
NDVI	6/8/2022	0.12
RSWIR	6/8/2022	0
NDWI	30/6/2023	0
MNDWI	30/6/2023	0
NDMI	30/6/2023	0.09
NDVI	30/6/2023	0
RSWIR	30/6/2023	0

Accuracy Assessment

Evaluating the reliability and precision of remote sensing data is an essential process that establishes the informational value and utility of the derived data products for end-users. Effective and informed decision-making depend on geospatial data is only feasible when the quality and accuracy of the data are well-understood.

The fundamental premise underlying all accuracy assessment methodologies is to compare the estimated or mapped values against reference data representing the true ground conditions, and to quantify the degree of correspondence or discrepancy between the two. In the specific context of land cover classification from remote sensing imagery, the 'estimated' values correspond to the land cover classes assigned to each pixel, while the 'reference' or 'ground truth' represents the actual land cover type present in the areas corresponding to those pixels. The primary emphasis in selecting pixels for accuracy assessment was on areas that could be unambiguously identified and verified on both the Landsat 8 imagery as well as high-resolution reference data from sources such as Google Earth and Google Maps.

The classification accuracy of remotely sensed data is typically depicted through an error matrix. Numerous researchers have advocated for the use of an error matrix to represent accuracy and recommend it as the standard reporting convention [20].

The precision of the classified images is evaluated based on (1) producer's Accuracy, (2) user's Accuracy, (3) overall Accuracy, and (4) Kappa coefficient (K) for each image.

The producer's accuracy is defined can be expressed as (Eq. 6):

$$\text{Producer's Accuracy} = \frac{\text{Correctly Classified Samples}}{\text{Total referenced Samples(column total)}} * 100 \quad (6)$$

The user's accuracy is defined as the ratio of correctly classified samples to the total classified samples can be expressed as (Eq. 7):

$$\text{User's Accuracy} = \frac{\text{Correctly Classified Samples}}{\text{Total classified Samples(The row total)}} * 100 \quad (7)$$

The overall accuracy indicates the proportion of the total number of correctly classified samples to the total number of samples, which can be expressed as (Eq. 8).

$$\text{Over all accuracy (V)} = \frac{\text{Correctly Classified Samples (Diagonal)}}{\text{Total Number Of Reference Samples}} * 100 \quad (8)$$

The three types of accuracies are quantified as a proportion.

The Kappa statistic quantifies the amount of information present in the primary diagonal of the error matrix, while also accounting for the level of agreement that could occur randomly. The Kappa coefficient can be expressed mathematically using the following equation (Eq. 9):

$$\text{Kappa coefficient (K)} = \frac{(\text{TS} * \text{TCS}) - \text{Z}}{\text{TS}^2 - \text{Z}} \quad (9)$$

where TS= Total number of Samples in a row, TCS = sum of correctly classified samples(Diagonal), and Z= sum of the product of all the samples in a row and all the samples in a column[21].

Relative percentage: It is the difference between the water area that is obtained from indices maps and the water area that is calculated from reference map divided by the water area that is calculated from reference map can be expressed as (Eq. 10):

$$\text{R.P} = \frac{(\text{A1} - \text{A2})}{\text{A2}} * 100 \quad (10)$$

R.P=Relative percentage

AI= Area of water from indices map

A2=Area of water from reference map

RESULTS AND DISCUSSIONS

The Landsat 8 OLI data are used to calculate five different water indices , namely (NDWI, MNDWI, NDVI, NDMI, RSWIR) then classified into three land cover/land-use categories (water, plant, land cover). Each Index yielded distinct outcomes, both in terms of classification precision and spatial metrics. The subsequent sections display the results obtained from this study and analyze them qualitatively and quantitatively.

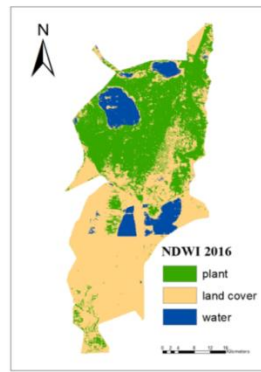
Qualitative Analysis of Visual Inspection

The water indices classifier was utilized in order to observe and map the changes in temporal land cover/land-use between 2016 and 2023 for AL-Hawizeh marsh. The set of maps were obtained and will be compared with real images from the Google Pro website or with false color composite image.

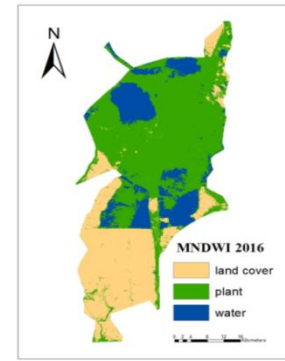
Five distinct land cover maps in (Fig. 3) are generated from the 30 m spatial resolution image using the MNDWI, NDWI, NDVI, NDM land RSWIR classifiers.



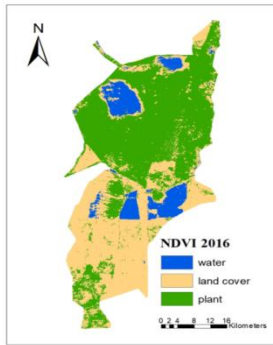
Reference 2016



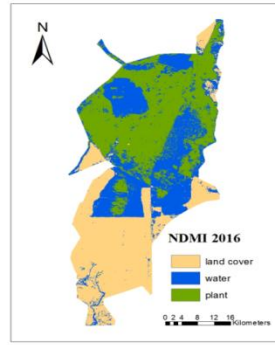
NDWI 2016



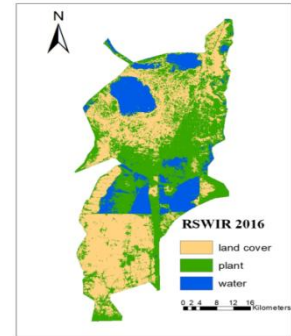
MNDWI 2016



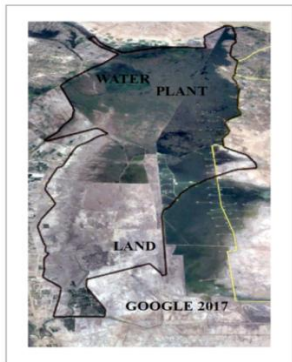
NDVI 2016



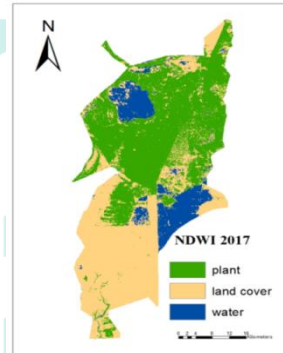
NDMI 2016



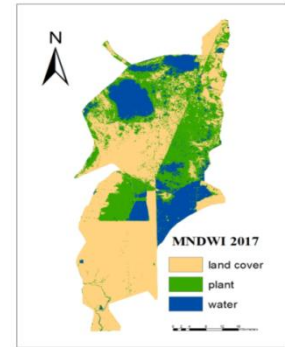
RSWIR 2016



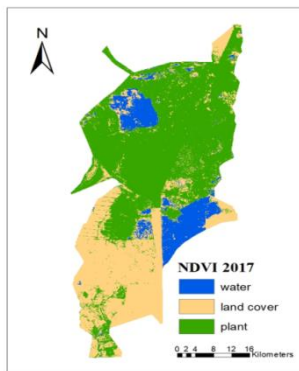
Reference 2017



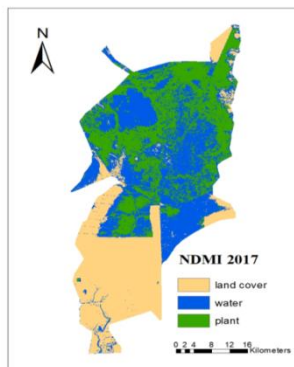
NDWI 2017



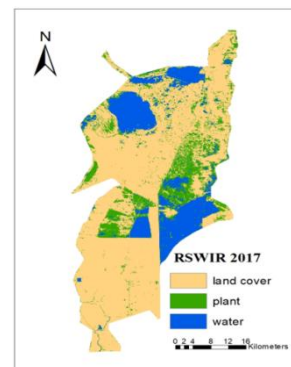
MNDWI 2017



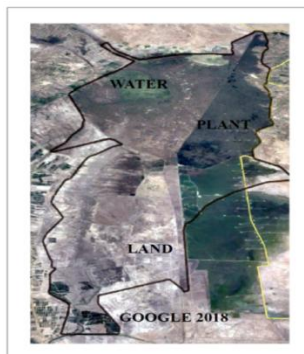
NDVI 2017



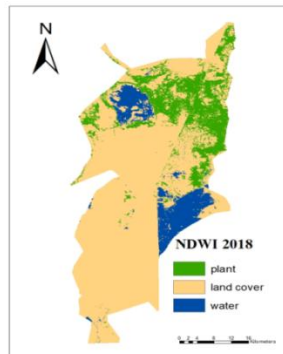
NDMI 2017



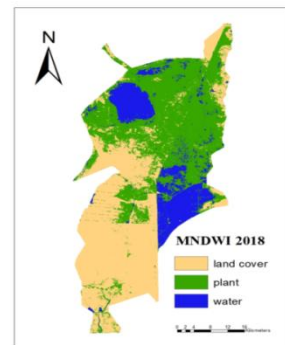
RSWIR 2017



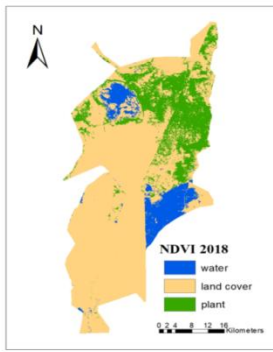
Reference 2018



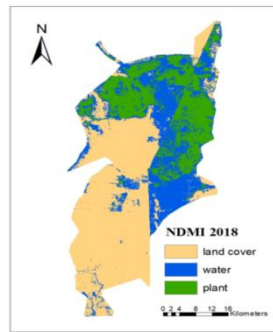
NDWI 2018



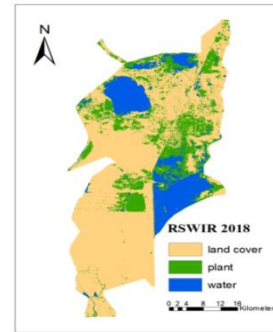
MNDWI 2018



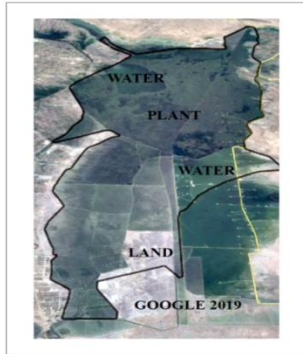
NDVI 2018



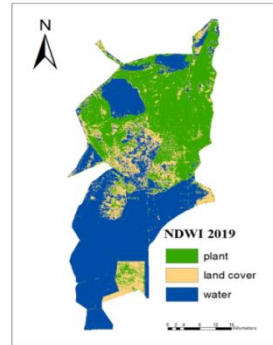
NDMI 2018



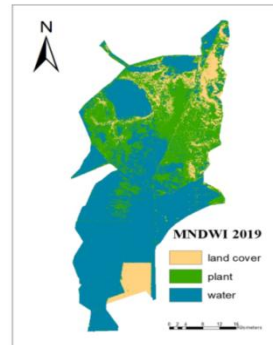
RSWIR 2018



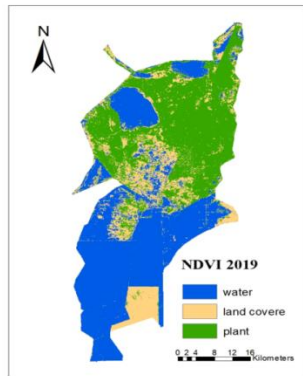
Reference 2019



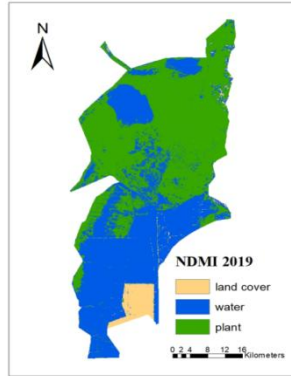
NDWI 2019



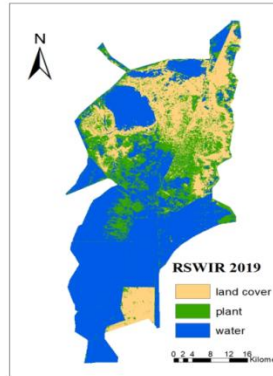
MNDWI 2019



NDVI 2019



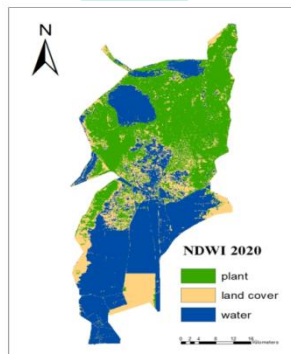
NDMI 2019



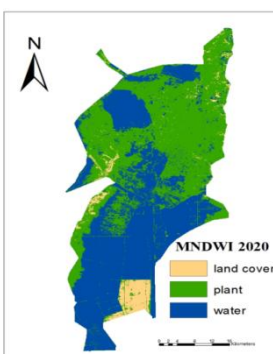
RSWIR 2019



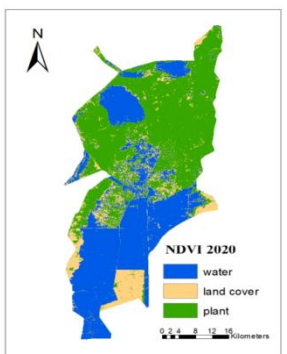
Reference 2020



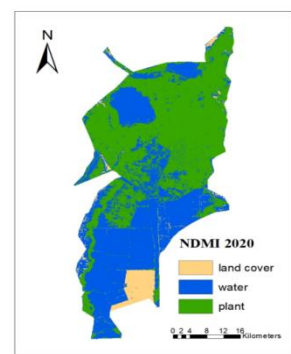
NDWI 2020



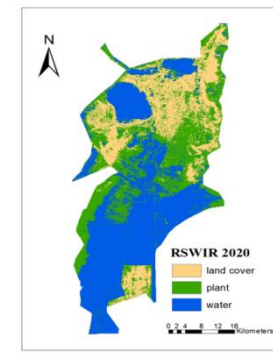
MNDWI 2020



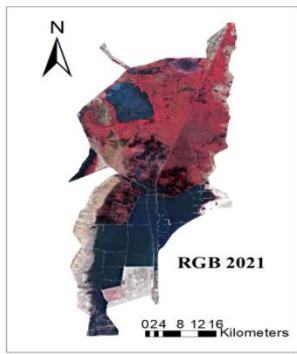
NDVI 2020



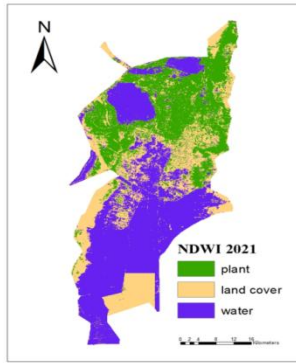
NDMI 2020



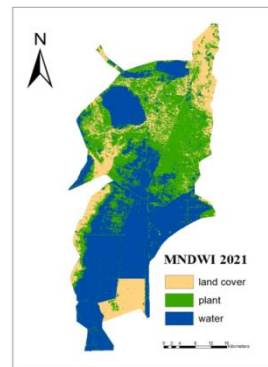
RSWIR 2020



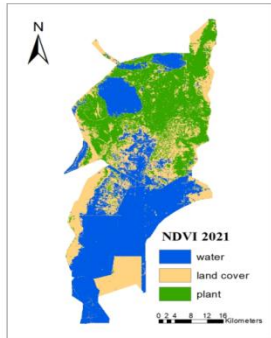
Reference 2021



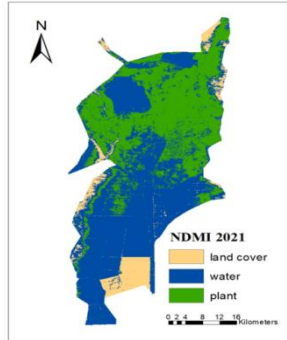
NDWI 2021



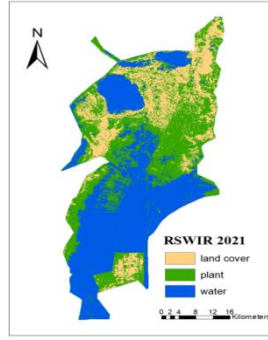
RSWIR 2021



NDVI 2021



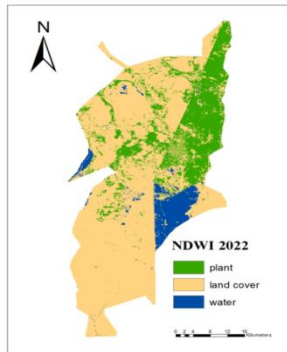
NDMI 2021



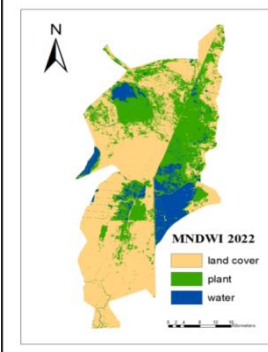
RSWIR 2021



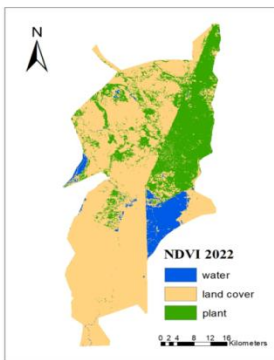
Reference 2022



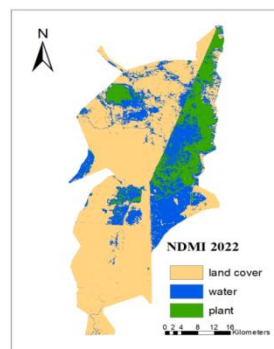
NDWI 2022



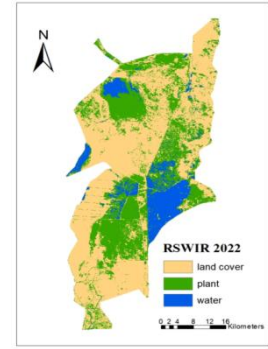
MNDWI 2022



NDVI 2022



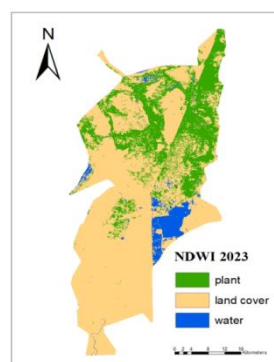
NDMI 2022



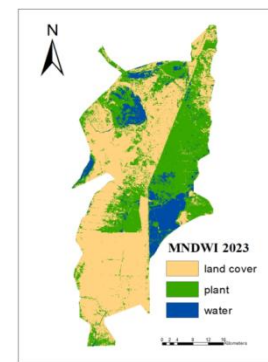
RSWIR 2022



Reference 2023



NDWI 2023



MNDWI 2023

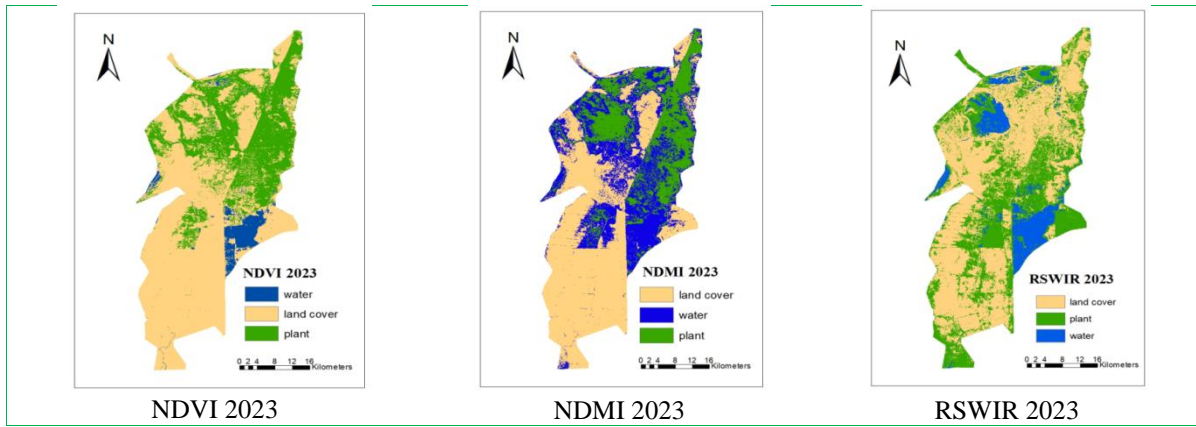


Fig. 3 Land cover/land-use maps obtained from Landsat 8 data using MNDWI, NDWI, NDVI, NDMI, RSWIR Classifiers for period from 2016 to 2023

All maps that have been produced by indices classifiers along with maps from Google pro website except map of (2021, 2022, 2023) that are compared with composite image RGB (false color composite B8, B4, B3) due to unavailability, the comparison is based on Google pro and composite image as a reference.

Through this comparison, the index NDWI can define the water region perfectly from 2016 to 2023, which is quite similar to the NDVI to determine water surface, vegetation and land cover region however, in 2019 NDVI indicates the vegetation areas less than the NDWI, the reason behind this could be the bad condition of vegetation (unhealthy) or the plants zone is not intensity as a result the reflectance of the plants for the Near Infra-Red is going to be reduced.

MNDWI effectively delineates flooded areas. The difference in reflectance between green and short wave Infra-Red (SWIR) is very small that could vanish in chaotic atmospheric condition such as those present during floods. This situation may cause the Modified Normalized Difference Water Index (MNDWI) to incorporate vegetation data, leading to an exaggeration of the extent of inundated area [9].

The estimation of MNDWI for the inundated area is very close to the RSWIR which depends on the difference of reflectance between red and short wave Infra-Red as such difference is very high while the MNDWI estimated for vegetation and land cover was good and very near to reference image.

The ability of RSWIR to specifies the water surface is almost perfect but not sufficient in regard of plants estimation .The effectiveness of RSWIR To recognize between vegetation and land cover is increased in dry condition as noticed in 2018, 2022, 2023 which are drought years considered.

NDMI works as an estimated of moisturized land cover ,which is unable to recognize plants and water surface clearly giving a large area of inundated region more than other indices because even the shallow and hydrated areas are being classified as inundated landscape. NDMI efficiency is risen during either high dry condition as seen in 2018, 2022, 2023 or floods season as in 2019 and 2020.

Quantitative Evaluation of Accuracy Numerical Comparison

Table 4 Overall Accuracy%

Year	NDWI	MNDWI	NDVI	NDMI	RSWIR
2016	90	95	89	88.33	69.23
2017	90.47	93.33	86.44	85	68.5
2018	82.8	91.9	86.15	76.66	69.23
2019	85	87.09	86.66	88	76
2020	78.33	89.55	91.9	92.53	76
2021	78.57	78.18	84.32	80.32	63.63
2022	73.77	79.62	87	79.31	61
2023	83.87	81.66	90.3	83.63	61
Average	82.85	87.04	87.72	84.22	68.07

Table 5 Kappa Coefficient

Year	NDWI	MNDWI	NDVI	NDMI	RSWIR
2016	0.8519	0.917	0.824	0.8229	0.5168
2017	0.8467	0.8916	0.7832	0.7755	0.5096
2018	0.698	0.87	0.7373	0.6166	0.5229
2019	0.7564	0.7824	0.7824	0.809	0.6036
2020	0.6542	0.8336	0.8658	0.8788	0.6158
2021	0.7223	0.6642	0.7622	0.7013	0.4279
2022	0.5631	0.6787	0.7824	0.63	0.3752
2023	0.72	0.7013	0.8432	0.736	0.3694
Average	0.7265	0.7923	0.7975	0.7462	0.492

n this comparison, as show in the (Tables 4) and (Tables 5) the overall accuracy , kappa coefficient and Relative percentage for NDWI, MNDWI, NDVI, NDMI, RSWIR classifier was (over all accuracy 82.85%, 87.04%, 87.72%, 84.22%, 68.07%) (kappa 0.7265, 0.7923, 0.7975, 0.7462, 0.492) respectively. Although RSWIR have the lowest overall accuracy among five indices , all these overall accuracies are considered relatively high, particularly for NDWI and NDVI indices with 87.07% and 87.72% respectively.

The variation in overall accuracy for the land cover maps derives from Landsat 8 can be attributed to the average resolution of the taken image and the underlying analysis performed for each index. Of the five classification indices evaluated, the results indicate that one index outperformed the others in terms of accurately mapping land cover features. However, it is important to note that the choice of index may depend on the specific objectives and characteristics of the study area. Further investigation is required to get deeper insight into the strengths and limitations of each index and to determine the most appropriate approach for land cover mapping using Landsat 8 data, the RSWIR provided the minimum accuracy and kappa with 68.07% , 0.492 so that RSWIR not suitable for classification.

The MNDWI produced the higher overall accuracy and kappa 87.04% and 0.7923 so that the best index for classification is MNDWI.

CONCLUSION

This study showcases the vast capabilities of remote sensing technology in assessing and monitoring the dynamics of water resource status. The findings reveal that Al-Hawizeh marsh experienced significant surface area variations from 2016 to 2023, with near-complete drying observed in 2018, 2022, and 2023. We found out that the water surface of Al-Hawizeh marsh is predominantly influenced by interannual rainfall variability, which is affected by climate fluctuations. Additionally, subsurface modifications and tunneling Work to the rivers feeding Al-Hawizeh marsh are an important factor requiring further study.

The paper shows that remote sensing is an appropriate technique for delineating water resources, even in diminutive and superficial aquatic environments.

The analysis of the analysis suggests that the Landsat 8-OLI dataset holds significant promise for creating detailed maps and tracking changes in water resources, and the MNDWI is the most effective index for this purpose. We recommend that the approach utilized in this study should be adapted to evaluate and track the dynamic changes in wetland water resource conditions, contingent upon the availability of suitable satellite data.. This will enable water resource managers to acquire the necessary information for optimizing sustainable management and conservation efforts.

REFERENCES

1. Karpatne, A., Khandelwal, A., Chen, X., Mithal, V., Faghmous, J., & Kumar, V. (2016). Global monitoring of inland water dynamics: State-of-the-art, challenges, and opportunities. In J. Lässig, K. Kersting, & K. Morik (Eds.), *Computational Sustainability* (pp. 121–147). Cham: Springer International Publishing.
2. Feyisa, Gudina L., et al. "Automated Water Extraction Index: A new technique for surface water mapping using Landsat imagery." *Remote sensing of environment* 140 (2014): 23-35.
3. Zhu, Lingli, et al. "A review: Remote sensing sensors." *Multi-purposeful application of geospatial data* 19 (2018).
4. Yurteri, Cansu, And Türker Kurttaş. "Determination of surface temperature in water bodies with the use of multiband landsat satellite images: Case study of Seyfe Lake." *Sigma Journal of Engineering and Natural Sciences* 41.6 (2023): 1144-1156.
5. Rouse, John Wilson, et al. "Monitoring vegetation systems in the Great Plains with ERTS." *NASA Spec. Publ* 351.1 (1974): 309.
6. McFeeters, S.K. The use of the normalized difference water index (NDWI) in the delineation of open water features. *Int. J. Remote Sens.* 1996, 17, 1425–1432.
7. Xu, Hanqiu. "Modification of normalised difference water index (NDWI) to enhance open water features in remotely sensed imagery." *International journal of remote sensing* 27.14 (2006): 3025-3033.
8. Wilson, Emily Hoffhine, and Steven A. Sader. "Detection of forest harvest type using multiple dates of Landsat TM imagery." *Remote Sensing of Environment* 80.3 (2002): 385-396.
9. Memon, Akhtar Ali, et al. "Flood monitoring and damage assessment using water indices: A case study of Pakistan flood-2012." *The Egyptian Journal of Remote Sensing and Space Science* 18.1 (2015): 99-106
10. Al-Mamalachy, Yousif, and Zeyad Al-Saedi. "Analysis and detection of inundation in al-hammar and central marshes/southern iraq using google earth engine." *Iraqi Bulletin of Geology and Mining* 18.1 (2022): 77-87.
11. AHMED, Bushra A., and Tabarak S. HASHESH. "Using satellite images classification to estimate water level in the southern Marshlands after the floods wave." *International Journal of Applied Sciences and Technology* 4.4 (2022): 194-205.
12. Hasab, H. A., et al. "Landsat TM-8 Data for retrieving salinity in AL-HUWAIZAH marsh, south of IRAQ." *J. Teknol* 75.1 (2015): 201-206.
13. Maarof, Bashar F., et al. "Geographical Assessment of the Natural Environment at Al-Huwaizah Marsh, Eastern of Misan Governorate (Iraq)." (*Humanities, social and applied sciences*) *Misan Journal of Academic Studies* 22.46 (2023): 293-310.
14. Seaton, Dylan St Leger. "The use of remote sensing data to monitor pools along non-perennial rivers in the Western Cape, South Africa." (2019).
15. Schroeder, Todd A., et al. "Radiometric correction of multi-temporal Landsat data for characterization of early successional forest patterns in western Oregon." *Remote sensing of environment* 103.1 (2006): 16-26.
16. Al-Quraishi, Ayad MF, Heman A. Gaznayee, and Mattia Crespi. "Drought trend analysis in a semi-arid area of iraq based on normalized difference vegetation index, normalized difference water index and standardized precipitation index." *Journal of Arid Land* 13 (2021): 413-430.

17. Xu, Hanqiu. "Modification of normalised difference water index (NDWI) to enhance open water features in remotely sensed imagery." *International journal of remote sensing* 27.14 (2006): 3025-3033.
18. Rokni, Komeil, et al. "Water feature extraction and change detection using multitemporal Landsat imagery." *Remote sensing* 6.5 (2014): 4173-4189.
19. Xie, Huan, et al. "Evaluation of Landsat 8 OLI imagery for unsupervised inland water extraction." *International Journal of Remote Sensing* 37.8 (2016): 1826-1844.
20. Congalton, Russell G. "A review of assessing the accuracy of classifications of remotely sensed data." *Remote sensing of environment* 37.1 (1991): 35-46.
21. Ashtekar, Avinash S., M. A. Mohammed-Aslam, and Ali Raza Moosvi. "Utility of normalized difference water index and GIS for mapping surface water dynamics in sub-upper Krishna Basin." *Journal of the Indian Society of Remote Sensing* 47 (2019): 1431-1442.

